QUANTIFICATION OF FACTORS AFFECTING THERMALLY-INDUCED BOW IN A CANDU FUEL ELEMENT SIMULATOR

by

P.M. MATHEW*, S. BASET**, J. VEEDER** AND E. KOHN***

*Atomic Energy of Canada Limited
Whiteshell Laboratories
Pinawa, Manitoba R0E 1L0

**Atomic Energy of Canada Limited
Chalk River Laboratories
Chalk River, Ontario K0J 1J0

***Ontario Hydro
700 University Avenue
Toronto, Ontario M5G 1X6

ABSTRACT

Thermally induced bow, caused by a circumferential temperature distribution around a fuel element, was investigated in this study using a fuel element simulator. The objective was to identify the factors affecting CANDU® fuel element bow induced by dryout as a result of some predicted reactor transients in which the maximum fuel temperature reaches 600°C. The results showed that circumferential temperature distribution, pellet-to-sheath mechanical interaction and creep were the major factors affecting bow. Transient bow increased with increasing diametral sheath temperature difference and with mechanical interaction between the pellet and the sheath. Permanent bow of the fuel element was observed in some tests which was the result of creep. Mechanical interaction between the sheath and pellet produced the stresses necessary for creep deformation. A simplified ABAQUS model was developed to explain the experimental findings and could be used to predict the bow behaviour of fuel elements during reactor transients, where the dry patches are of different sizes.

INTRODUCTION

This paper addresses thermally induced bow, caused by a circumferential temperature gradient around a fuel pin. If one side of the fuel element becomes hotter than the other then the element bows in the direction of the hotter side to accommodate the differential axial strain. The magnitude of the deflection caused by this mechanism is called "transient bow". If the sheath is

---

stressed and stress relaxation occurs some permanent deflection will remain on removal of the temperature gradient, and this is called "permanent bow".

Under normal operating conditions, temperature variations around the fuel element are caused by non-uniform coolant temperatures resulting from imperfect mixing, non-uniform heat transfer between sheath and coolant resulting from variations in subchannel geometry, and from asymmetric heat generation in the fuel in response to neutron flux gradients across an element. Permanent bow was observed in Zircaloy-sheathed Douglas Point reactor fuel and to a greater extent in high temperature Zr-2.5 Nb-sheathed WR-1 fuel [1,2]. Analysis of those results showed that neutron flux gradients and mechanical interaction between the fuel and sheath were the dominant factors in element bowing.

The major factors causing bow in dryout are: circumferential temperature gradient, sheath-to-pellet mechanical interaction and stress relaxation. This study was conducted to quantify the effects of the parameters described above on both transient and permanent bow as a result of a short period of dryout of a fuel element during which the maximum sheath surface temperature reaches approximately 600°C with the cooler side of the sheath remaining at about 300°C. This scenario would produce a circumferential temperature gradient around a fuel element, and therefore the necessary conditions for the element to bow. To achieve this objective small-scale out-reactor tests using a fuel element simulator with a circumferential temperature gradient were conducted and the tests modelled with a commercially available code ABAQUS [3].

EXPERIMENTAL DETAILS

An experimental facility and a fuel element simulator were designed and built for this study. The general concept for the experimental design was to use a fuel element simulator with unirradiated UO_2 pellets having an off-set hole inside a Pickering-type fuel sheath. The off-set hole contained a heater and the heater power could be controlled. The fuel element simulator was contained inside a stainless-steel chamber and was supported at the two ends. Helium gas was purged around the simulator to produce the desired circumferential temperature distribution. The bow of the element at the centre was measured with a Laser device.

Test Facility. Figure 1 shows the components of the test facility. It consists of a test chamber, Laser head, gas supply system, power supply and a data acquisition system. Based on heat transfer calculations, a fuel sheath-to-coolant heat transfer coefficient of about 300 $W/m^2{\bullet}K$ is required to achieve the desired temperature distribution in the fuel element simulator. The heat transfer coefficient depends on several factors, such as the coolant medium, its pressure, velocity and temperature. Calculations showed that a flow tube, with an I.D. of 22.1 mm surrounding the fuel element simulator carrying helium gas at 0.5 MPa with a flow velocity of 15-20 m/s, would provide the necessary conditions in the flow tube to achieve the desired heat transfer coefficient. Therefore, the facility was designed for those conditions.

The test chamber, shown schematically in Figure 1, is a stainless steel vessel housing the fuel element simulator as shown in Figure 2. The test section is 0.25 m long and is the centre part. The simulator test section is supported at both ends with a set of three centering pins, that would allow free axial expansion and rotation of the simulator. A flow tube (see Figure 2) surrounding the simulator has a quartz optical window at the top centre, through which bow measurements are made with a Laser device. Helium gas enters one end of the test chamber from the gas supply system (see Figure 1) at 0.5 MPa through a system of pressure regulators and a pressure relief valve. The gas enters the annulus between the flow tube and the fuel element simulator and exits at the other end. At the outlet end the flow rate is monitored with a flow rotometer.

A 100 KVA transformer, operating at 26 V maximum output, supplied power to the heater. Manual or automatic power controls were used in the tests. For a typical bow test the power used was approximately 1800 watts, corresponding to about 20 volts and 90 amps. The transient bow and the sheath temperatures were measured during the test. For the sheath temperature measurements spot-welded thermocouples were used. The temperature readings were corrected for helium cooling based on results from calibration tests. The permanent bow of the simulator was measured after cooling to room temperature using a laser device and confirmed with a dial gauge.

Fuel Element Simulator. Fuel element simulators with Pickering-type CANLUB-coated fuel sheath and pellets were used. The O.D. of the pellets and the I.D. of the sheaths were selected to vary the diametral gap between the pellet and the sheath. The gap controls the degree of mechanical interaction. Three groups of diametral gaps were tested in this study:

Group 1: 0.014 to 0.020 mm diametral gap
Group 2: 0.004 to 0.008 mm diametral gap
Group 3: 0.082 mm diametral gap.

The pellets had an off-set hole of about 4 mm diameter, 4.6 mm from the centre. They were pushed into the sheath by applying a uniform load. A flexible tungsten-26% rhenium heater, insulated with thoria tubes of short lengths, was placed inside the off-set hole. The simulator was instrumented and positioned centrally inside the test chamber and the electrical power cables were connected for testing.

Test Procedure. Tests with different circumferential temperature gradients were conducted with a constant target fuel element bottom temperature of 300°C. This was achieved by controlling the helium flow velocity and the power input. The top and bottom fuel element simulator temperatures and the bow were monitored as a function of time and the permanent bow was measured after the test. To determine the influence of holding time on bow at temperature, in selected tests, the simulator was held at temperature for up to 600 s and transient measurements were carried out during that period. The permanent bow was measured after the test.

MODEL DEVELOPMENT

A simplified ABAQUS model was developed to support the experiments. The sheath was modelled as a simply supported beam free to expand and rotate at its ends. The 4-node ABAQUS shell element was chosen to model the experimentally observed non-linear temperature distribution around the circumference. The pellet-to-sheath interaction was accounted for through a gap model in a subroutine which simulated the pellet expansion. By assuming symmetry of loading, temperature and boundary conditions about both the vertical axis and the mid-span of the sheath, only one quarter of the sheath was required to be modelled. A total of 180 elements were used with 18 circumferential and 10 axial elements. The creep deformation was modelled using standard creep strain relationship for the Zircaloy α-phase.

Because the mechanical interaction between the pellets and the sheath on fuel element bow is not fully understood, a simplified approach similar to that used by Veeder and Schankula [1] was adopted. If the pellets grip the sheath tightly without slippage it will force the sheath to elongate and the differential strain will be equal to the difference in thermal strain between the fuel and the sheath. It is well known that UO_2 expands more than the sheath. Any decrease in differential strain resulting from plastic or creep strain is accounted for in the model. The interaction stress is calculated from the stress-strain relationship. The interaction stress is converted to an equivalent body force and is implemented in the ABAQUS model with a grip factor, G, which is introduced to account for no-slip or full grip (G = 1) and slip (G = 0) conditions.

Exact values of the factor G can be obtained only by modelling the complete pellet/sheath assembly in a coupled thermal/mechanical analysis. Even though no such extensive analysis was conducted in this study, a simplified approach was adopted to monitor the closure of the radial gap between the pellet and the sheath in a separate subroutine. In this gap model the fuel pellet is initially assumed to touch the sheath at the lower point and the initial gap between the sheath and the pellet is assumed to be a cosine function of the radial angle from the sheath centre. As the temperature increases the pellet expands more than the sheath and the gap closes. This gap-closure process is monitored and when the gap vanishes the pellet is assumed to grip the sheath fully (G = 1). Therefore, for a small initial gap, full grip conditions apply early in the transient at most of the surface and no significant difference in bow would be expected between the no-slip or full grip case and the gap model. For a larger initial gap, full grip conditions could develop during the transient as the gap closes during the heatup. Such a situation could lead to a different bow than expected from full grip and slip conditions.

RESULTS AND DISCUSSION

The results from the ABAQUS model showed that a linear temperature distribution in the sheath with respect to the diameter, does not produce any axial stresses. For non-linear temperature distributions, the stresses are non-zero. For the temperature boundary conditions in this study, the stresses caused by temperature alone are too small to cause significant plastic deformation. The stresses required for plastic deformation are provided by the mechanical interaction between the pellet and the sheath.

The experimental results from two tests with the initial gaps of 0.004 and 0.082 mm are compared with the modelling results here. In Figure 3 the results for a diametral gap of 0.004 mm are shown. The top graph shows the measured fuel element top and bottom temperatures in open symbols and the corrected temperatures from calibration tests as closed symbols. The corrected temperatures were used for computations. The bottom graph in Figure 3 shows the measured bow as open circles, as a function of time for the same test. The observed bow is directly proportional to the temperature difference between the top and bottom fuel element temperatures. The modelling results are superimposed on this figure. The lowest curve in Figure 3 is the result of computations for slip and creep conditions. The next higher curve is for full-grip and no-creep conditions. The calculated curve above that is the result from the gap-closing model under full-grip conditions. The computational results, shown with closed circles, are for full-grip and creep conditions. The experimental results show a permanent bow of about 0.75 mm. Only the model with mechanical interaction and creep can explain this finding. The high transient bow observed in this test, is explained only if mechanical interaction is accounted for. Although it was possible to fit the model to the experiments by selecting a grip factor between 0 and 1, this was not done. Comparison of the modelling results given by the top two curves in Figure 3 shows, as expected, that for a small gap of 0.004 mm the bow calculated by the gap closure mechanism does not differ significantly from full-grip condition.

In Figure 4 results of a test with a large diametral gap of 0.082 mm are shown. The top graph in this figure shows the top and bottom measured and corrected fuel element temperatures. A comparison of the computational results with the measured bow is shown in the bottom graph. The modelling results from full-grip and creep conditions (top curve in Figure 4, bottom) overpredict the test results. The experimental results can be bound by the calculated curves for slip with creep and full-grip with the gap-closure model and creep. The obtained permanent bow was small, but negative compared to the positive trend for the smaller gap. Only the gap model could explain the observed negative permanent bow. A comparison of the transient bow from Figures 3 and 4 shows that high mechanical interaction leads to high transient and permanent bows.

In Figure 5 the transient bow, measured during the first 20 s of hold period, is plotted against the top-to-bottom fuel element temperature difference for the three groups of tests with different diametral gaps. The experimental trend for the three groups of diametral gaps is shown as a straight line in this figure. The results show that high mechanical interaction between the pellet and the sheath leads to high bows. It should be noted that in our experiments the bow measured is for a span length of 0.25 m. In practice, the dryout patches in a CANDU bundle are smaller in postulated accidents. The irradiated pellets are generally cracked and therefore the mechanical interaction is expected to be less. As a result, the bow observed from these tests are expected to be significantly higher than in practice.

Of interest in this study is the permanent bow after a short dryout period. In Figure 6 the permanent bow is plotted against top-to-bottom temperature difference for three different diametral gaps. The results show that permanent bow is negative for a large gap, but it is positive and increases with temperature difference for smaller gaps. If a temperature difference of about 150°C is exceeded, permanent bow could result. This indicates that for the test conditions creep deformation may become significant at temperatures greater than 450°C.

CONCLUSIONS

The experimental facility and the fuel element simulator developed here was used to quantify the different factors affecting bow, such as top-to-bottom temperature difference, mechanical interaction between pellet and sheath and creep. Transient bow increases with top-to-bottom temperature difference and mechanical interaction. Permanent bow is caused by creep and the stresses required for plastic deformation are produced by the mechanical interaction. The model developed with ABAQUS can explain the test results.

Further study aimed at enhancing the understanding of the bowing behaviour of CANDU multi-elements in dryout is reported in a companion paper [4] presented at this conference.

ACKNOWLEDGEMENTS

Financial support from the CANDU Owners Group, consisting of Atomic Energy of Canada Limited, Ontario Hydro, Hydro Quebec and New Brunswick Power, is gratefully acknowledged.

REFERENCES

1. VEEDER, J., and SCHANKULA, M., "Bowing of Pelletized Fuel Elements: Theory and In-Reactor Experiments," Nuclear engineering and Design 29 (1974) 167-179.

2. WALKER, J.F. and NICKOLSON, A.M., "The Irradiation Behaviour of WR-1 Fuel," Atomic Energy of Canada Limited Report, WNRE-34, 1971.

3. "ABAQUS/Standard User's Manual - Version 5.4," HKS Inc. 1994.

4. KOHN, E., HU, R.H., HADALLER, G.I. and FORTMAN, R.A., "Understanding CANDU Fuel Bowing in Dryout: An Industry Approach," paper presented at this Conference.

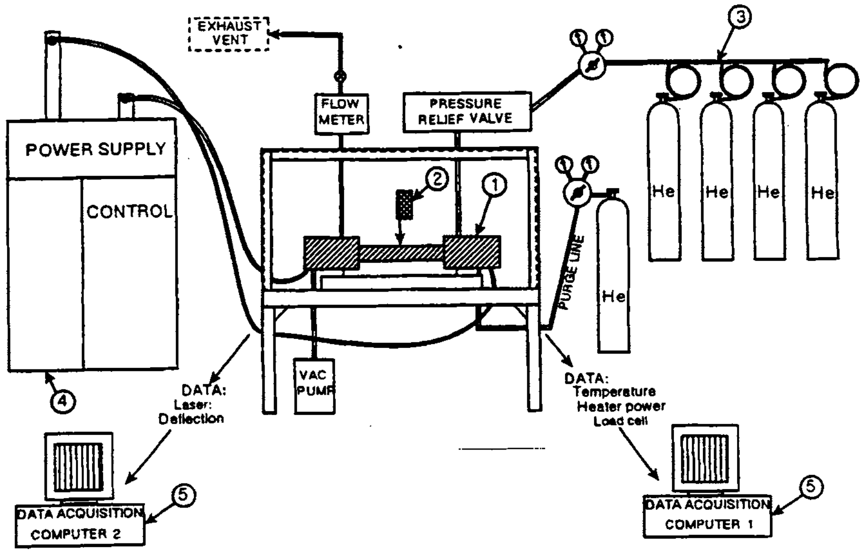

FIGURE 1: COMPONENTS OF THE BOW TEST FACILITY: 1) BOW TEST CHAMBER, 2) LASER HEAD, 3) GAS SUPPLY SYSTEM, 4) POWER SUPPLY, 5) DATA ACQUISITION SYSTEM

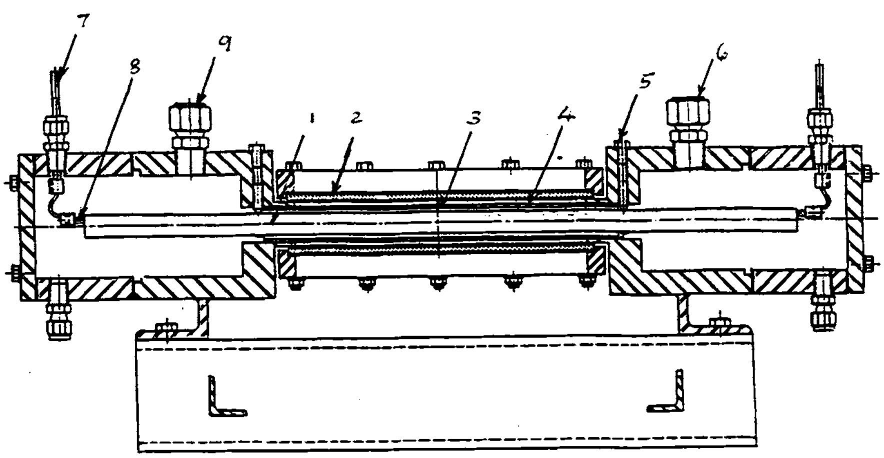

FIGURE 2: BOW TEST CHAMBER: (1 = FUEL ELEMENT SIMULATOR, 2 = QUARTZ WINDOW, 3 = OPENING FOR BOW MEASUREMENT, 4 = FLOW TUBE, 5 = SUPPORT PINS, 6 = He INLET, 7 = POWER CABLE, 8 = HEATER WIRE, 9 = HELIUM OUTLET)

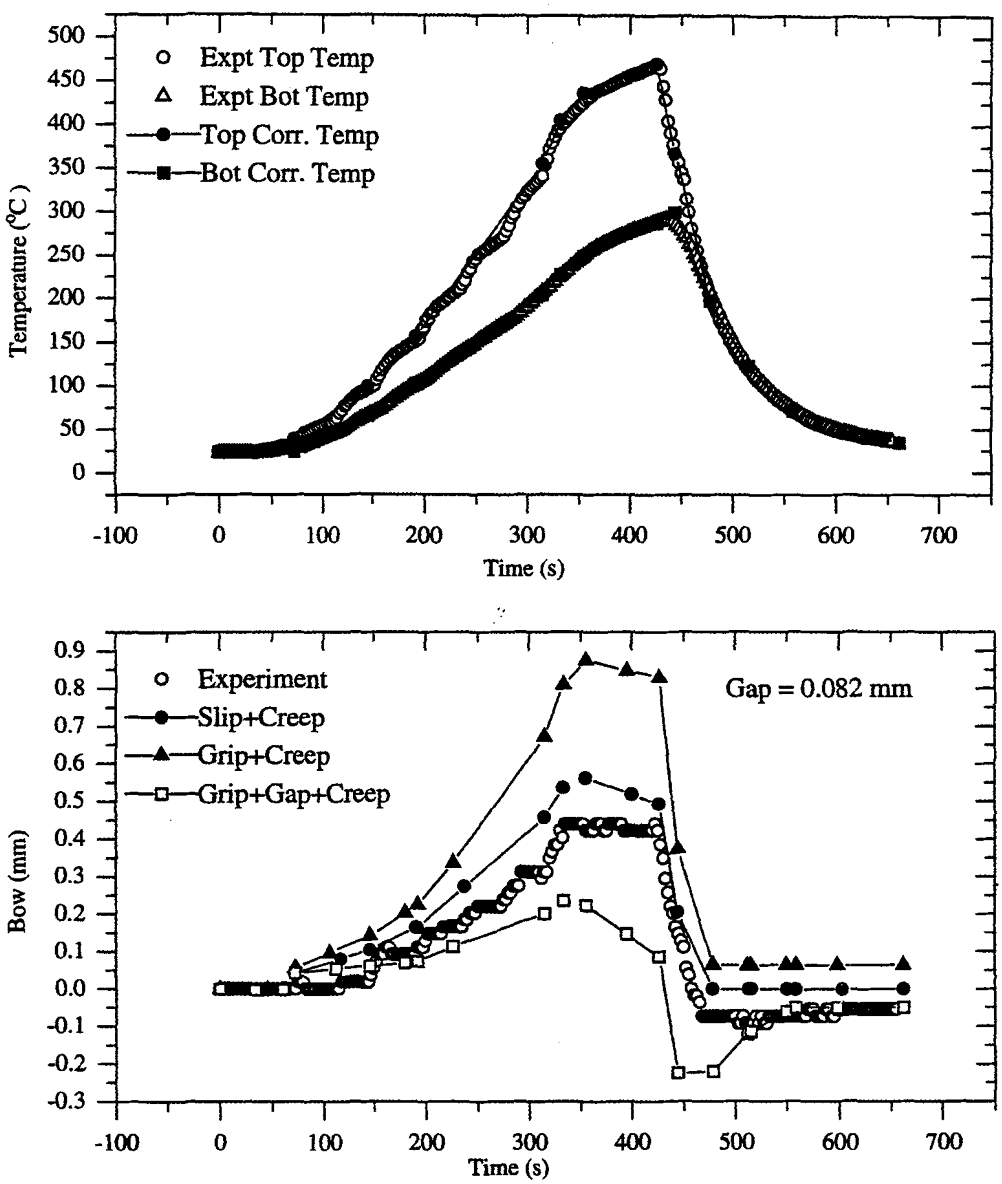

FIGURE 4: LINEARIZED TEMPERATURE-TIME CURVE (SOLID LINES) USED AS INPUT TO ABAQUS MODEL (TOP) AND A COMPARISON OF THE MODEL PREDICTIONS WITH THE MEASURED BOW FOR A BOW TEST WITH A LARGE DIAMETRAL GAP OF 0.082 mm

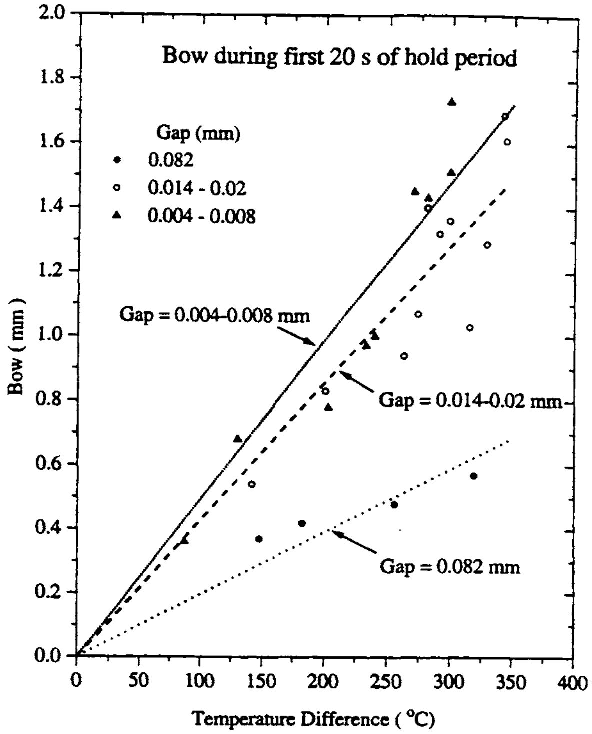

FIGURE 5: RELATIONSHIP BETWEEN AVERAGE TOP-TO-BOTTOM TEMPERATURE DIFFERENCE AND BOW DURING THE FIRST 20 s AT TEMPERATURE. THREE GROUPS WITH DIFFERENT DIAMETRAL GAPS ARE IDENTIFIED.

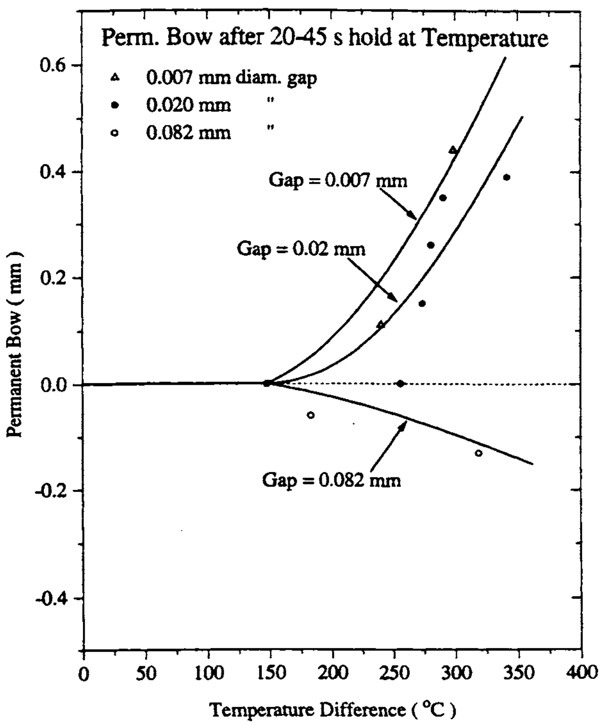

FIGURE 6: PERMANENT BOW AFTER 20-45 s HOLD AT TEMPERATURE AS A FUNCTION OF GAP SIZE